Physiological responses of *Oxyrrhis marina* to a diet of virally infected *Emiliania huxleyi*

Andrew G. Goode[1,2], David M. Fields[1], Stephen D. Archer[1] and Joaquín Martínez Martínez[1]

[1] Bigelow Laboratory for Ocean Sciences, East Boothbay, ME, United States of America
[2] School of Marine Sciences, University of Maine, Orono, ME, United States of America

ABSTRACT

The coccolithophore *Emiliania huxleyi* forms some of the largest phytoplankton blooms in the ocean. The rapid demise of these blooms has been linked to viral infections. *E. huxleyi* abundance, distribution, and nutritional status make them an important food source for the heterotrophic protists which are classified as micro-zooplankton in marine food webs. In this study we investigated the fate of *E. huxleyi* (CCMP 374) infected with virus strain EhV-86 in a simple predator-prey interaction. The ingestion rates of *Oxyrrhis marina* were significantly lower (between 26.9 and 50.4%) when fed virus-infected *E. huxleyi* cells compared to non-infected cells. Despite the lower ingestion rates, *O. marina* showed significantly higher growth rates (between 30 and 91.3%) when fed infected *E. huxleyi* cells, suggesting higher nutritional value and/or greater assimilation of infected *E. huxleyi* cells. No significant differences were found in *O. marina* cell volumes or fatty acids profiles. These results show that virally infected *E. huxleyi* support higher growth rates of single celled heterotrophs and in addition to the "viral shunt" hypothesis, viral infections may also divert more carbon to mesozooplankton grazers.

INTRODUCTION

Cell lysis, due to viral infection, accounts for up to 30% of daily mortality rates of marine microorganisms (*Suttle, 1994*; *Van Hannen et al., 1999*), influences shifts in microbial community structure (*Martínez Martínez et al., 2006*; *Thingstad, 2000*), and is hypothesized to result in the reduction of infected eukaryotic phytoplankton's net primary productivity (*Suttle, 1994*) while increasing the overall ecosystem's net primary productivity (*Weitz et al., 2015*). Conventional dogma holds that virus-induced cell lysis diverts energy away from the traditional food web by releasing the organic carbon (C), nitrogen (N), and phosphorus (P) in phytoplankton cells to the dissolved phase, fueling an active bacterial population. This process, known as the "viral shunt", is hypothesized to transfer 6–26% of C (estimated 150 gigatons of C per year) from photosynthetic plankton to the dissolved organic pool (*Suttle, 2005*; *Wilhelm & Suttle, 1999*). However, to the best of our knowledge,

the magnitude of the C "shunt" during viral infection has not been directly measured. A quantitative understanding of the pathways and factors that affect the flow of organic C in marine systems is key to understanding community structure and for predicting resource availability to support important commercial species. Although it is known that viral infection of algal cells alters crucial cellular and biogeochemical processes (*Evans, Pond & Wilson, 2009*; *Gilg et al., 2016*; *Malitsky et al., 2016*; *Rosenwasser et al., 2014*; *Suzuki & Suzuki, 2006*), the impacts of these changes on the nutritional value of cells and on the grazing and growth rates of both micro- and macrozooplankton are largely unexplored (*Evans & Wilson, 2008*; *Vermont et al., 2016*).

The coccolithophore *Emiliania huxleyi* is a globally distributed and abundant oceanic phytoplankton species whose blooms can cover thousands of square kilometers (*Holligan et al., 1993*). They are a key component in pelagic food webs contributing essential amino acids and fatty acids (FA) to the base of the food chain, which are crucial for supporting multiple cellular functions and growth in higher trophic level organisms. The collapse of *E. huxleyi* blooms has been linked to infection by double-stranded (ds) DNA viruses (EhVs) (*Bratbak, Egge & Heldal, 1993*; *Brussaard et al., 1996*; *Wilson et al., 2002*). Infection with EhV causes rapid physiological changes in *E. huxleyi* that divert host resources toward virus replication and assembly; e.g., decreased photochemical efficiency (*Gilg et al., 2016*) and altered metabolic pathways such as glycolysis, FA, and nucleotide biosynthesis (*Evans, Pond & Wilson, 2009*; *Malitsky et al., 2016*; *Rosenwasser et al., 2014*). Within three hours post inoculation with EhV, *E. huxleyi* cultures shift from producing polyunsaturated (PUFA) to monounsaturated (MUFA) and saturated (SFA) fatty acids (*Floge, 2014*). Additionally, viral infection can increase the uptake capacity of N and P by expressing viral genes which code for nutrient transporters not found in the host's genome and increase access to diverse nutrient sources unavailable to uninfected cells (*Monier et al., 2017*; *Monier et al., 2012*; *Wilson, Carr & Mann, 1996*). High P and/or N resources are critical for optimal viral proliferation in phytoplankton hosts (*Maat & Brussaard, 2016*; *Maat et al., 2016*; *Mojica & Brussaard, 2014*; *Monier et al., 2017*), including *E. huxleyi* (*Bratbak, Egge & Heldal, 1993*; *Martínez Martínez, 2006*). At the scale of large oceanic *E. huxleyi* blooms it remains unclear if the sum of viral alterations enhances or diminishes the overall amount of C and essential nutrients that are passed to higher trophic levels.

Predation by heterotrophic and mixotrophic protists (microzooplankton) dominates grazing on phytoplankton in aquatic microbial food webs, and plays a key role in C cycling and nutrient regeneration (*Calbet & Landry, 2004*; *Sherr & Sherr, 2002*; *Sherr & Sherr, 2009*; *Strom et al., 2001*). The heterotrophic dinoflagellate *Oxyrrhis marina* has been shown to preferentially graze on EhV-infected *E. huxleyi* cells, relative to uninfected cells (*Evans & Wilson, 2008*). Although the mechanism driving this preferential grazing is unclear, *Evans & Wilson (2008)* proposed possible changes in prey size, motility, nutritional value, palatability, and chemical cues as potential causes. However, to the best of our knowledge, those results have not yet been reproduced in any independent studies. Also, one aspect that was not investigated is *if* and *how* preferential grazing on infected *E. huxleyi* might modify the transfer of C and essential nutrients through the food web. In this study we investigated the effect of viral infection on the growth and ingestion rates, cell volume,

and FA composition of *O. marina* cells to better understand how the grazing behavior and physiology of microzooplankton is influenced by viral infection of abundant and important phytoplankton prey.

MATERIALS AND METHODS

Culture maintenance

Clonal *Emiliania huxleyi* strain CCMP 374 (non-axenic, non-calcifying; 3-5μm) and non-axenic clonal *O. marina* strain CCMP 1795 were obtained from the Provasoli-Guillard National Center for Marine Algae and Microbiota (NCMA-Bigelow Laboratory, Boothbay, ME, USA). A non-axenic clonal *Dunaliella* sp. strain was sourced from the University of South Carolina. *E. huxleyi*, *O. marina,* and *Dunaliella* cultures were maintained at 16 °C under a light:dark cycle (14:10 h; 250 μmol photons m^{-2}s $^{-1}$). *E. huxleyi* and *Dunaliella* sp. cultures were kept in exponential growth phase by periodically transferring 10% (v/v) culture into fresh f/2-Si seawater medium (*Guillard, 1975*). Under these standard culture conditions *E. huxleyi* CCMP 374 cultures display near-synchronous division that starts approximately 1 h before the onset of the light period and last approximately 4 h (*Gilg et al., 2016*). *O. marina* stock cultures were fed weekly with fresh *Dunaliella* sp. cultures (5% (v/v)). Fresh EhV-86 (*Wilson et al., 2002*) lysates were obtained by inoculating *E. huxleyi* cultures in exponential growth phase. Once culture clearance was observed (typically 3–5 days post inoculation (p.i.)), cell debris was removed by filtration (0.45 μm PES filter) and the EhV-86 lysates were then stored at 4 °C in the dark for up to two weeks prior to being used in an experiment. The same EhV-86 lysate stock was used to determine infection dynamics and for grazing experiments 1–3 (see experimental details in the sections below). Cell and virus concentrations were measured using a FACScan flow cytometer (Beckton Dickinson, Franklin Lakes, NJ, USA), equipped with an air-cooled laser providing 50 mW at 488 nm with standard filter set-up, as previously described (*Brussaard, 2004*; *Marie et al., 1999*). Virus particles and bacteria cells were enumerated from 1 ml 0.5% glutaraldehyde-fixed (final concentration) samples that were frozen in liquid nitrogen and stored at −80 °C until further processing. The samples were thawed and stained with SYBR Green I prior to flow cytometry (FCM) enumeration. Virions and bacteria were discriminated based on green fluorescence and side scatter signals (Fig. S1A). *Emiliania huxleyi* and *O. marina* cells were visualized and enumerated together from fresh, non-fixed 1 ml samples by triggering the cytometer on red fluorescence. Cells were enumerated based on chlorophyll red auto-fluorescence and side scatter (Figs. S1B, S1B, S1D). Note that red fluorescence in fed *O. marina* cells derived from ingested prey (Figs. S1C, S1D). Starved *O. marina* cells only show residual red fluorescence signal (Fig. S1B).

Emiliania huxleyi virus infection dynamics

Fifty milliliter aliquots of exponentially growing *E. huxleyi* culture were inoculated at four EhV-86 to host ratios of 5:1, 20:1, 50:1, and 100:1, in triplicate. The inoculations both here and for experiments 1–5 (see below) were timed to coincide with the end of the cytokinesis to minimize the effect of division on the estimation of infection and grazing rates. Fresh f/2-Si media was added to each flask in order to achieve the same *E. huxleyi*

cell concentration in all flasks. One milliliter aliquots were taken from each culture at 2, 4, 6, and 20 h p.i. for cell enumeration using flow cytometry (FCM). Cells were stained with the orange fluorescent lipid-specific dye N-(3-Triethylammoniumpropyl)-4-[4-(dibutylamino)styryl] pyridinium dibromide (FM 1-43; Invitrogen Co., Carlsbad, CA, USA) to allow discrimination between visibly infected and non-infected *E. huxleyi* cells (*Martínez Martínez et al., 2011*) (Fig. S2). Progression of the viral infection was quantified by tracking the percentage of visibly infected *E. huxleyi* over time.

Emiliania huxleyi C and N content

A 150 ml volume of *E. huxleyi* culture in exponential growth phase was divided in two equal volumes. One of the aliquots received 45 ml EhV-86 to achieve a 50:1 virus:host ratio; the second one received an equal volume of fresh f/2-Si medium to achieve similar cell concentration in both cultures. *Emiliania huxleyi* concentration and percentage of visibly infected cells in each flask was determined immediately after the addition of EhV-86 and f/2-Si medium and at 5 h p.i., and at 24 h p.i. Six 5 ml samples were taken from each flask immediately after the addition of EhV-86 and f/2-Si medium and at 24 h p.i. and were gravity filtered through a combusted glass fiber filter (Whatman GF/F; GE Healthcare Life Sciences, Pittsburg, PA) to collect particulate matter. The filtrates were then passed through fresh combusted GF/F filters to serve as C and N background controls (residual dissolved C and N retained by the filters). Filters were stored at −80 °C until analysis. Prior to testing, the filters were dried at 45 °C for 24 h before being placed in 9× 10 mm Costech tin capsules using clean forceps and sample preparation block. Calibration standards were prepared from acetanilide. The samples, standards, and filter blanks were analyzed using a Costech ECS 4010 elemental analyzer (980 °C combustion).

Oxyrrhis marina specific growth and grazing rates

Five independent experiments (experiments 1–5) were performed. *Oxyrrhis marina* was not fed for 3 days prior to each experiment to ensure their feeding vacuoles were empty. FCM was employed to check for the absence of prey-derived chlorophyll red autofluorescence signal within *O. marina* vacuoles after the 3-day period. For experiments 1–4, stock non-axenic *E. huxleyi* cultures ($\sim$1 $\times$ 10^6 cells ml^{-1}) were split into two equal volumes. One of the flasks was inoculated with fresh EhV-86 lysates to achieve the virus:host ratios specified for each experiment in Table 1. Incubations were carried out for 6 h to allow sufficient viral infection levels (see results from virus infection dynamics below, Fig. 1). The second flask received f/2-Si media equal to the virus stock volume to match the dilution of cells. For experiment 5, *E. huxleyi* culture was infected as described previously and was split into two equal volumes at 6 h p.i. One aliquot was kept unfiltered and the other one was filtered through a 0.4 μm pore size polycarbonate filter. The filter pore size was tested prior to the experiment to ensure selective removal of *E. huxleyi* cells (<1% cells passed through). Between 78% and 100% bacteria and 75–95% EhVs were allowed through the 0.4 μm filter. Experiment 5 was conducted to determine if *O. marina* growth rate is augmented or supported by ingested bacteria, virions, and/or dissolved organic matter (DOM) within the infected cultures. Non-infected diet was not included in experiment 5.

Table 1 Details of experiments performed.

	Experimental conditions					Parameters measured (Om)			
	EhV: Eh ratio	% infected Eh cells 6 h p.i.	Eh:Om ratio	Initial Om (cells/ml)	Duration (days)	Growth rate	Grazing rate	Fatty acids	Cell vol
Experiment 1	100:1	20	30:1	6000	0.25		x		
Experiment 2	100:1	20	100:1	4500	3	x	x	x	
Experiment 3	100:1	20	100:1	4000	7	x	o		
Experiment 4	50:1	36	100:1	6000	4	x	x		x
Experiment 5	50:1	34	100:1	6000	4	x	x		

Notes.
Eh, *Emiliania huxleyi*; Om, *Oxyrrhis marina*.
o indicates that the grazing rates were calculated using *E. huxleyi* k-values from non-grazing controls in experiment 2.
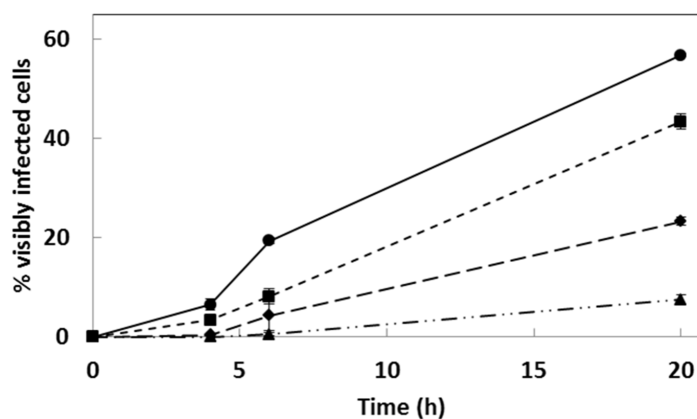

Figure 1 **Infection progression of *E. huxleyi*.** Infection progression of *E. huxleyi* at four different virus:host ratios; 5:1(▲), 20:1 (◇), 50:1 (■), and 100:1 (●). Values are mean percentage (%) of cells visibly infected over time (hours) ± one standard deviation.

Full-size 🖼 DOI: 10.7717/peerj.6722/fig-1

In all experiments, the flasks were incubated without shaking under the standard culture conditions indicated above. Equal volume aliquots of either infected (including 0.4 μm-filtered) or non-infected *E. huxleyi* cultures were fed to triplicate *O. marina* cultures. Both infected and non-infected food contained bacteria; additionally, the infected food contained free EhV particles. Additional aliquots of the *E. huxleyi* cultures (infected and non-infected) were maintained separately as non-grazing controls. It should be noted that non-grazing control cultures were not maintained during experiment 3, instead, average *E. huxleyi* growth rates from experiment 2 were used to normalize for *E. huxleyi* cell growth and lysis. Both these experiments employed the same EhV stock and virus:host ratio, and only differed in the length of time of the experiment (Table 1). We have shown in this study and elsewhere (*Gilg et al., 2016*; *Vermont et al., 2016*) that under comparable conditions, infection dynamics and virus production are highly reproducible. *E. huxleyi* and *O. marina* cell concentrations were monitored in each flask by FCM. Prey and predator

cell concentrations were measured immediately after the initial feeding and every 30 min for the first 2 h and then every hour up to 6 h for experiment 1 (Fig. S3) and every 24 h for experiments 2–5. During experiments 2–5 O. marina cultures were fed fresh prey immediately after determining cell concentrations at the end of each 24 h incubation period for a total of 3–7 days (Table 1). The duration of our experiments are ecologically relevant and representative of high rates of viral infection during induced blooms of mixed assemblies of E. huxleyi (Castberg et al., 2001; Martínez Martínez et al., 2007). The additions of fresh prey cells each day were calculated to bring the prey:predator ratio to the same level as at the beginning of the experiment. Sterile f/2-Si medium was added, as needed, to the O. marina cultures to maintain comparable cell concentration between treatments. Additional experimental design information can be found in Table 1. Oxyrrhis marina specific growth and grazing rates were determined by the equations of Frost (1972) and used to calculate O. marina growth per E. huxleyi cell consumed.

Projected *O. marina*'s abundance

Our goal in these experiments was to maintain consistent concentration of O. marina and E. huxleyi throughout the experiment. At each time point the cultures were sampled and high concentration aliquots of fresh E. huxleyi cultures were added to replace the cells that were ingested or lost due to mortality. The concentration data with the daily dilution was used to calculate the total number of O. marina and E. huxleyi cells that were produced and consumed, respectively, over the duration of the experiment. Average growth and grazing rates of individual cultures from experiments 2–4 ($n = 9$) were combined to calculate the overall average ± 1 standard error (SE) growth and grazing rates of O. marina fed either infected or non-infected E. huxleyi cells. We postulated a starting population size of 6,000 O. marina cells and assumed E. huxleyi prey saturation and no mortality for O. marina over a 7-day period. We applied the overall O. marina's average ± 1 SE growth rate over the 7-day period to calculate the cumulative population size supported by infected or non-infected E. huxleyi. We then used the calculated average population size of O. marina and its average grazing rates (±1 SE) (Frost, 1972) to calculate the total ingestion of E. huxleyi cells at each time point.

Oxyrrhis marina and *E. huxleyi* fatty acid (FA) analysis

The effect of feeding on virally infected or non-infected E. huxleyi on the FA composition of O. marina was investigated during experiment 2. For FA analysis, 5 ml aliquots were taken from non-infected E. huxleyi cultures and from cultures 6 h after inoculation with EhV-86 (in duplicate), as well as from O. marina cultures (in triplicate) before feeding them with E. huxleyi cells (Day 0) and after three days being fed E. huxleyi (Day 3). Samples were vacuum filtered through a combusted glass fiber filter (Whatman GF/F; GE Healthcare Life Sciences, Pittsburg, PA), and stored at −80 °C until analysis. FAs were converted to FA methyl esters (FAMEs) in a one-step extraction direct methanolysis process (Meier et al., 2006) following the procedures detailed in Jacobsen, Grahl-Nielsen & Magnesen (2012). FAMEs were analyzed on a gas chromatograph with mass spectrometric detector (Shimadzu GCMS-QP2010 Ultra; Shimadzu Scientific Instruments, Columbia, MD, USA).

FAME samples were reconstituted in 200 µl of hexane and 1 µl was injected into the GC/MS injector which was kept at 250 °C. FAMEs were separated on a SGE BPX-70 column, in a helium mobile phase at a flow rate of 1.17 ml min^{-1}. A Supelco 37 Component FAME Mix (47885-U; Supelco Analytical, Bellefonte, PA, USA) standard solution was used for instrument calibration. Individual FAMEs were identified via comparison to standard mixture peak retention times and fragmentation patterns using the NIST-library of compound mass spectra. FAME concentrations were calculated from peak area relative to that of a C19:0 internal standard that was added to each sample prior to extraction. FA type concentrations were converted to percentages of the combined total FA concentration.

Oxyrrhis marina cell volume

The cell size of *O. marina* was measured for starved cells (3 days) prior to the experiment and once a day for three days from each *O. marina* culture during the grazing experiment 4. The size of O. marina was measured on fixed cells. Common fixatives such as Lugol's or glutaraldehyde alter cell volume (*Menden-Deuer, Lessard & Satterberg, 2001*). Alternatively, live cells can be immobilized by adding nickel sulfate (0.003% final concentration) or 70% ethanol, which appears to have no effect on cell shape and size (*Menden-Deuer, Lessard & Satterberg, 2001*). We chose to fix *O. marina* cells by transferring 50% (v/v) into 70% ethanol and storing at 4 °C for 30 min prior to analysis. Ethanol did not appear to alter cell size since our results were very similar to the measurements with added nickel sulfate from *Menden-Deuer, Lessard & Satterberg (2001)*; however, no direct comparison of these two methods was carried out. Ten randomly selected individual *O. marina* cells from each aliquot were photographed on a hemocytometer. Width and length of the cells were measured using ImageJ (*Schneider, Rasband & Eliceiri, 2012*). Volume was calculated as a rotational ellipsoid; V= $\frac{\pi}{6}xd^2xh$ (*Edler, 1979*; *Menden-Deuer & Lessard, 2000*). Differences in cell volume between treatments were evaluated using a standard *t*-test. Total C per *O. marina* cell was estimated based on the average cell volume using the equation log pg C cell^{-1} = $-0.665 + \log \text{vol} \times 0.939$ (*Menden-Deuer & Lessard, 2000*).

Statistical analyses

Temporal differences within the same diet treatment for *E. huxleyi* C and N content and for *O. marina* specific growth and ingestion rates, and cell volume were analyzed with a two-tailed, paired *t*-test, Alpha level 0.01. When comparing parameters between treatments and for FA composition, the differences were analyzed with a two-tailed, unpaired *t*-test assuming equal variance, Alpha level 0.01. *P*-values ($P < 0.05$) were significant and $P < 0.01$ were considered highly significant.

RESULTS

Emiliania huxleyi virus infection dynamics

The percentage of visibly infected cells (as revealed by FCM) increased at higher virus:host inoculation ratios over a 20 h period. During this same period cell abundance did not change significantly in virally-infected cultures compared to non-infected cultures (Fig. S2C). The highest virus:host ratio (100:1) yielded at least 20% visibly infected *E. huxleyi* cells by 6 h p.i.,

Goode et al. (2019), *PeerJ*, DOI 10.7717/peerj.6722

7/25

and ∼57% by 20 h p.i. (Fig. 1); consequently we chose this ratio for experiments 1–3, which were carried out with the same EhV-86 stock and under the same environmental conditions employed to determine the infection dynamics (Fig. 1). The infection dynamics of *E. huxleyi* (CCMP374) and viral (EhV-86) production are highly consistent and reproducible when using the same host and virus strains and conditions, in particular when using the same virus lysate stock within a 4-week time frame (*Gilg et al., 2016*; *Vermont et al., 2016*). Infected cells begin to release virus progeny at around 4.5 h p.i. (*Mackinder et al., 2009*) and any cells not infected by the initial EhV inoculum can become infected during successive infection rounds by the new EhV progeny. At the high virus:host ratios used in this study, previous work has shown that 70%–100% of the *E. huxleyi* cells become infected by 24 h p.i. (*Gilg et al., 2016*; *Vermont et al., 2016*), even if not evident by FCM (*Martínez Martínez et al., 2011*). In experiments 4 and 5, we used fresh EhV-86 lysate stocks that yielded an apparent higher percentage of infected cells by 6 h p.i. than the EhV-86 stock used in the three preceding experiments. Consequently, we reduced the initial virus:host ratio to 50:1 virus:host ratio to achieve more comparable infection dynamics (∼36% and ∼34% of *E. huxleyi* cells were visibly infected by 6 h p.i. in experiments 4 and 5, respectively).

Emiliania huxleyi C and N content

Staining with the lipid-specific dye FM 1-43 showed ∼15% visibly-infected *E. huxleyi* cells by 5 h p.i. and over 70% visibly-infected cells by 24 h p.i. Over a 24 h incubation, both infected and non-infected cultures of *E. huxleyi* exhibited a slight but significant increase ($P = 4.94 \times 10^{-4}$ and $P = 0.018$, respectively) in C content of 9.27 ± 0.19 to 10.86 ± 0.43 pg C cell^{-1} ($\pm$SD) for infected cells and 8.94 ± 0.94 to 10.42 ± 0.26 pg C cell^{-1} for non-infected cells, respectively. Carbon content was not statistically different between treatments ($P = 0.420$ at t0 and $P = 0.057$ at t24) (Fig. 2A, Table S1). *Emiliania huxleyi* N content was not statistically different between samples at the beginning of the experiment ($P = 0.989$), but it increased significantly over the 24 h incubation; from 1.51 ± 0.08 to 1.89 ± 0.13 pg N cell^{-1} ($\pm$SD) ($P = 6.36 \times 10^{-4}$) for infected cells and 1.51 ± 0.05 to 2.09 ± 0.07 pg N cell^{-1} ($P = 1.80 \times 10^{-5}$) for non-infected cells, respectively. The N content of non-infected cells was significantly higher after the 24 h incubations ($P = 0.008$) (Fig. 2B).

Oxyrrhis marina specific growth rate

The 6 h duration of experiment 1 was too short to measure *O. marina* growth rates. In the longer experiments (experiments 2–4), the growth rates of *O. marina* ranged from 0.28 to 0.43 day^{-1} (average 0.35 ± 0.08 day^{-1} ($\pm$SD)) when fed non-infected prey and from 0.47 to 0.56 day^{-1} (average 0.52 ± 0.05 day^{-1}) when fed infected prey (Fig. 3A, Table S2). Specifically, *O. marina* specific growth rates were 30% ($P = 0.002$), 43.4% ($P = 5.29 \times 10^{-6}$), and 91.3% ($P = 0.006$) higher when fed infected *E. huxleyi* during experiments 2, 3, and 4, respectively (Fig. 3A). Based on the average growth rates, and assuming no loss term for *O. marina* cells, we calculated the abundance of *O. marina* cells after 7 days was 233% higher on a diet of infected cells than on non-infected *E. huxleyi* cells (Fig. 3D). In a follow up experiment (experiment 5) that measured the ingestion and growth rates
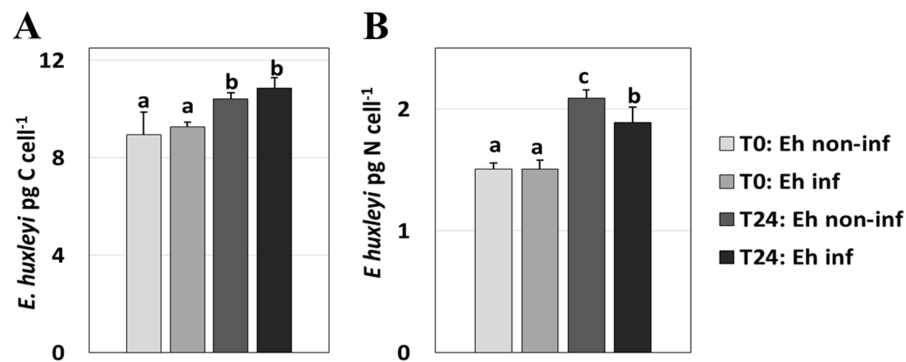
Figure 2 **_E. huxleyi_ C and N concentration.** *E. huxleyi* C (A) and N (**B**) concentration (pg cell $^{-1}$) at 0 and 24 hours p.i. Values are mean $\pm$ one standard deviation. Letters indicate statistical similarity. Same letters indicate no statistical difference between compared treatments and different letters denote significant statistical differences.

Full-size ⊡ DOI: 10.7717/peerj.6722/fig-2

of *O. marina* on infected *E huxleyi* and bacteria, the data showed that the growth rate of *O. marina* was significantly higher ($P = 6.49 \times 10^{-4}$) when fed infected, non-axenic *E. huxleyi* cells (average 0.38 ± 0.02 day^{-1} ($\pm$SD)) than when fed <0.4 μm filtrate from infected cultures (average 0.10 ± 0.05 day^{-1} ($\pm$SD)) (Fig. 4A, Table S3).

Oxyrrhis marina ingestion rates

During the initial 1.9 h in experiment 1, *O. marina* ingestions rates were not significantly different ($P = 0.68$) when fed infected (14.48 ± 0.18 Eh cells Om^{-1} h^{-1} ($\pm$ SD)) versus non-infected cells (14.88 ± 1.57 Eh cells h^{-1}). Between 1.9 (experiment 1) and 6 h (experiment 2) no additional ingestion was measurable (Fig. 3B, Fig. S3, Table S2). Initial pulse-feeding following a period of starvation is commonly observed in grazing experiments and may explain the equal number of prey ingested in experiment 1 (1.5 h) and 2 (6 h). The combined results from grazing experiments 2–4 yielded ingestion rates that were on average 35.4% lower ($P = 0.001$) for *O. marina* fed infected (39.74 ± 12.14 Eh cells Om^{-1} day^{-1}) versus non-infected *E. huxleyi* cells (60.34 ± 10.13 Eh cells Om^{-1} day^{-1}) (Fig. 3B, Table S3). The higher total number of ingested *E. huxleyi* cells, both infected and non-infected, measured in experiments 2–4 versus experiment 1 indicated that *O. marina* can saturate its feeding vacuoles within the first 1.5 h of feeding and then resumes feeding after 6 h, as prey cells were digested. Also, the relatively low standard deviation values between experiments 2–4 indicated daily ingestion rates were fairly constant over time. Normalizing *O. marina* growth rate to the number of cells ingested renders differences between diets ($P = 1.60 \times 10^{-5}$) even more striking (i.e., 86.30%, 238.62%, and 154.44% higher growth rate when fed infected *E. huxleyi* cells, for experiments 2, 3, and 4 respectively) (Fig. 3C, Table S2). The elevated growth rate in of *O. marina* in the infected cultures was driven largely by ingestion of *E. huxleyi* cells and not from ingested bacteria within the cultures (Fig. 4). A comparison of the growth rates of *O. marina* feeding on infected cultures showed that when the *E. huxylei* cells were removed, *O. marina* growth rates decreased precipitously from 0.38 d^{-1} ($\pm$ 0.02 SD) to 0.1 d^{-1} ($\pm$ 0.05) (Fig. 4A). Ingestion rates
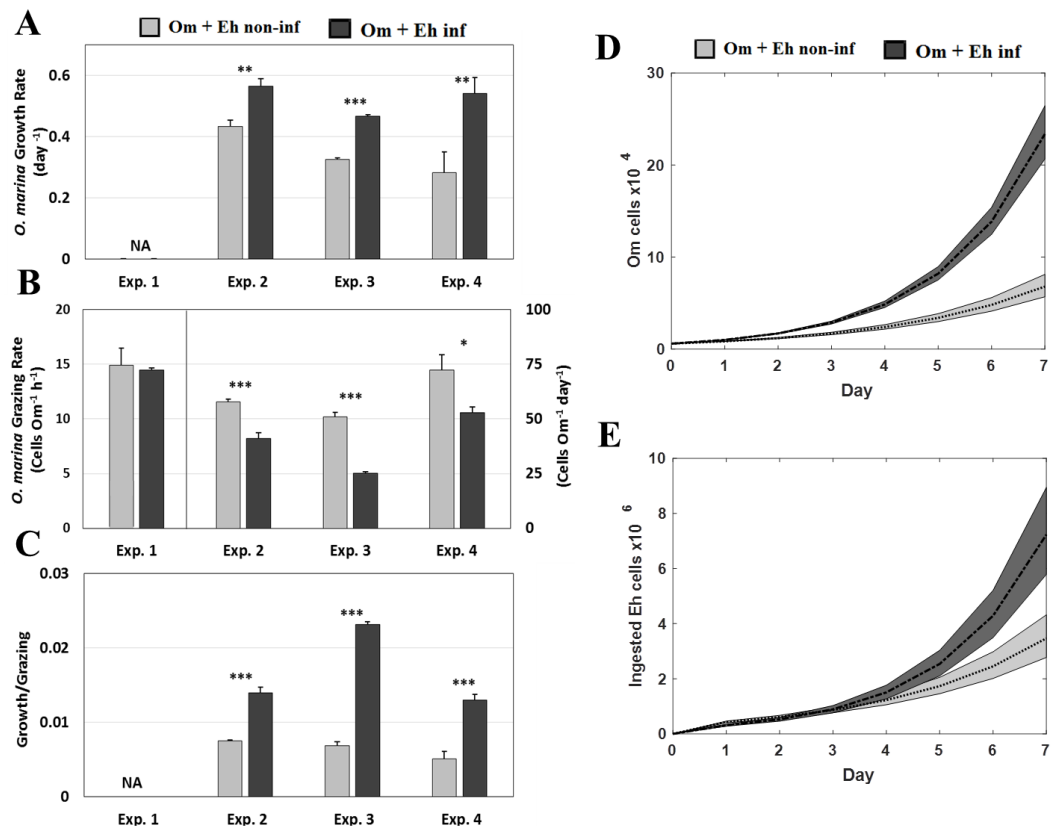
Figure 3 Growth and grazing rates. Differential growth and grazing rates of *O. marina* fed non-infected versus infected *E. huxleyi*. (A) *O. marina* growth rates (day^{-1}). (B) *O. marina* grazing rates (Eh cells Om$^{-1}h^{-1}$ (Exp. 1) or Eh cells Om^{-1} day^{-1} (Exps. 2–4); see Table 1). (C) *O. marina* growth rate divided by grazing rate (*O. marina* divided per *E. huxleyi* consumed). Values mean ± one standard deviation (Experiments 2, 3, and 4) and standard deviation (Experiment 1). (D) Projected *O. marina*'s population size at each time point. **E:** Projected total consumption of *E. huxleyi* cells at each time point. Dashed lines are average values and shaded regions are one standard error from Experiments 2, 3, and 4. Asterisks indicate statistical significance: *** $p < 0.001$, ** $p < 0.01$, * $p < 0.05$.

Full-size 🖾 DOI: 10.7717/peerj.6722/fig-3

of *O. marina* on infected *E. huxleyi* cells were similar to experiments 2–4 (64.98 ± 2.72 Eh cells Om^{-1} day^{-1}). However, in the <0.4 µm filtered treatment where approximately 99% of the *E. huxleyi* cells were removed, the ingestion of *E. huxleyi* decreased by 95%, (3.5 ± 4.04 Eh cells Om^{-1} day^{-1}) on day 1 and was undetectable on the subsequent 3 days (Fig. 4B, Table S3). Conversely, the ingestion of bacteria cells (Fig. 4C) in the flasks with high abundance of *E. huxylei* cells showed low ingestion rates of bacteria on day 1(262 ± 64.51 bact cells Om^{-1} day^{-1}) and no detectable ingestion on the subsequent days of the experiment. However, when the E huxleyi cells were removed, bacteria ingestion rates increased from 767 ± 130.35 bact cells Om^{-1} day^{-1} on day 1 to 3132 ± 455.02 bact cells Om^{-1} day^{-1} on day 4. Grazing of bacteria cells was statistically different ($P = 3.17 \times 10^{-3}$) between diets on day 1 (Fig. 4C, Table S3).

Combining the higher growth rate of *O. marina* (i.e., higher end abundance, Fig. 3D) and the average ingestion rates (Fig. 3B), we estimated that the total consumption of
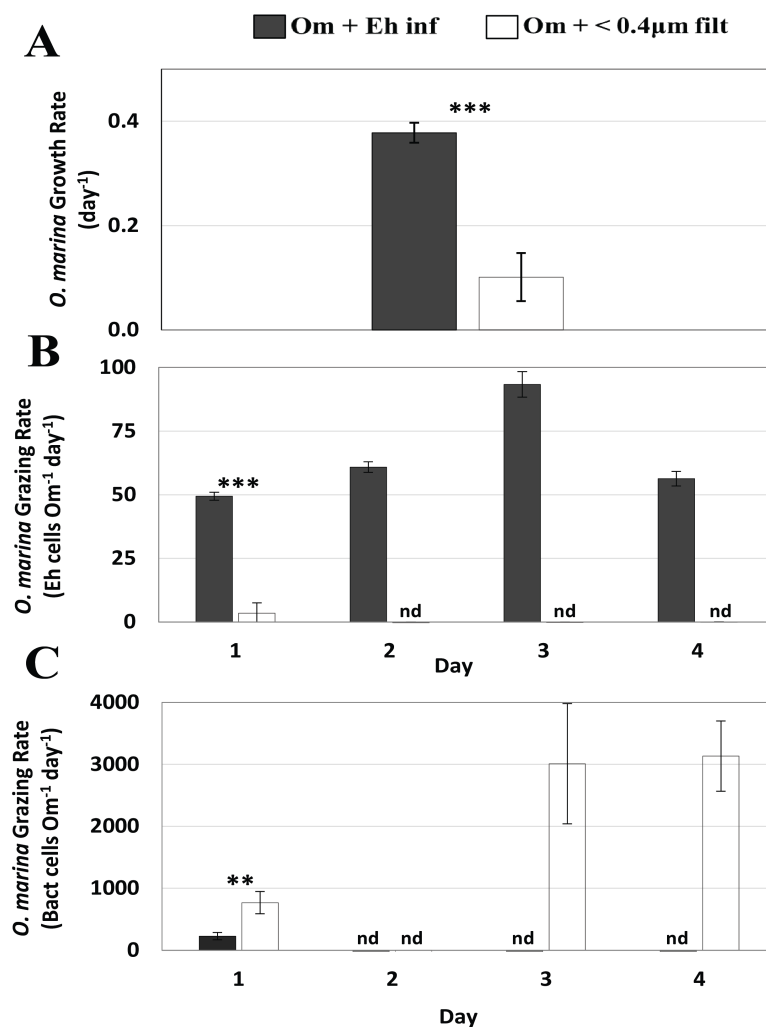
Figure 4 Differential growth and grazing rates measured in experiment 5 for *O. marina* fed non-axenic infected *E. huxleyi* versus < 0.4 μm filtrate of a non-axenic infected *E. huxleyi* culture. (A) *O. marina* growth rates (day^{-1}). (B) *O. marina* grazing of *E. huxleyi* cells (Eh cells Om^{-1} day^{-1}). (C) *O. marina* grazing of bacteria cells (Bact cells Om^{-1} day^{-1}). Values mean ± one standard deviation. nd denotes "none detected". Asterisks indicate statistical significance: ***$p < 0.001$, **$p < 0.01$.

Full-size ◪ DOI: 10.7717/peerj.6722/fig-4

virus-infected *E. huxleyi* cells would exceed that of non-infected cells after 4–5 days and would be on average 63.2% higher for virus-infected *E. huxleyi* over a 7-day period (Fig. 3E).

Oxyrrhis marina and *E. huxleyi* fatty acid analysis

Fatty acid (FA) profiles were similar between infected and non-infected cultures of *E. huxleyi* (note the low SD values between the concentrations of the most abundant FAs in the duplicate non-infected and duplicate infected *E. huxleyi* cultures). (Table 2). Similarly, minor differences in the FA profile were observed in *O. marina* that had consumed infected versus non-infected cells. The cultures containing *O. marina* fed infected *E. huxleyi*

Table 2 Percentage (%) of individual fatty acids to total FA concentration of cultures in which: (i) *O. marina* was depleted of prey at the start of the experiments (Day 0 Om); (ii) the *E. huxleyi* cultures fed to *O. marina*; (iii) after three days fed non-infected *E. huxleyi* (Om + Eh non-inf); and (iv) after 3 days fed infected *E. huxleyi* (Om +Eh inf). Values are mean ± one standard deviation, $n = 4$, $n = 4$, $n = 3$ and $n = 3$, respectively. Note the values for *E. huxleyi* are the average of duplicate non-infected and duplicate infected cultures.

	FA Class	Day 0 Om	*E. huxleyi*	Day 3 Om + Eh non-inf	Day 3 Om + Eh inf
SFA	C14:0	0.2 ± 0.2	0.2 ± 0.1	0.4 ± 0.1	1.2 ± 1.3
	C15:0	0.4 ± 0.3	0.3 ± 0.2	0.5 ± 0.0	0.8 ± 0.4
	C16:0	30.9 ± 4.5	27.6 ± 3.6	29.4 ± 7.6	24.6 ± 2.6
	C17:0	2.7 ± 0.1	2.7 ± 0.7	2.7 ± 0.3	3.2 ± 0.1[c,d]
	C18:0	36.2 ± 11.1	60.9 ± 7.6[a]	46.9 ± 6.4	56.4 ± 7.1[c]
	C20:0	1.1 ± 0.1	1.3 ± 0.3	1.5 ± 0.8	1.2 ± 0.4
	C22:0	0.8 ± 0.2	0.7 ± 0.6	3.3 ± 2.3	1.8 ± 0.9
	C24:0	0.7 ± 0.5	1.1 ± 0.1	0.6 ± 0.4	0.4 ± 0.3
MUFA	C16:1	0.8 ± 1.6	0.0	0.0	0.0
	C18:1(n-9cis)	5.0 ± 4.0	0.0[a]	1.6 ± 1.4[b]	1.6 ± 1.6[c]
	C18:1(n-9trans)	4.6 ± 3.3	0.0[a]	1.7 ± 1.5	1.3 ± 1.2
	C22:1	1.1 ± 0.9	0.1 ± 0.1	0.0	0.0
PUFA	C18:2	2.7 ± 1.4	0.0	0.0[b]	0.2 ± 0.3[c]
	C20:2	2.9 ± 2.3	5.0 ± 3.7	7.1 ± 1.9[b]	3.2 ± 1.3[c,d]
	C20:5 (n–3)	1.2 ± 1.2	0.1 ± 0.1	0.2 ± 0.3	0.3 ± 0.3
	C22:6 (n-3)	8.6 ± 7.7	0.0	4.0 ± 4.1	3.9 ± 3.3
	$\sum$ SFA	73 ± 15	95 ± 4[a]	86 ± 9	89 ± 6
	$\sum$ MUFA	12 ± 8	0.1 ± 0.1[a]	3 ± 3	3 ± 3
	$\sum$ PUFA	15 ± 8	5 ± 4	11 ± 6	8 ± 3

Notes.
a, Day 0 Om vs. *E.huxleyi*; b, Day 0 Om vs. Day 3 Om + Eh non-inf; c, Day 0 Om vs. Day 3 Om + Eh inf; d, Day 0 Om vs. Day 3 Om + Eh non-inf vs. Day 0 Om vs. Day 3 Om + Eh inf.

contained slightly higher proportions of C17:0 and 2-fold higher proportions of C20:2 (Table 2).

Oxyrrhis marina cell volume

The average volume of *O. marina* cells was slightly larger ($\sim$10%) when fed a diet of infected *E. huxleyi* prey ($5{,}226 \pm 1{,}267\ \mu m^3 (\pm SD)$) than when fed non-infected *E. huxleyi* ($4{,}706 \pm 1{,}259\ \mu m^3$). However, the difference was not statistically significant ($P = 0.21$) (Table 3, Fig. S4). While the SD were large, possibly due to the relatively low number of cells that were measured for each time point and treatment, they were similar for both diet treatments suggesting similar high volume variations between individuals in both treatments.

DISCUSSION

The results presented here show compelling evidence that virus-infected *E. huxleyi* fuels higher growth rates in the heterotrophic dinoflagellate *O. marina*. The data shows that the higher growth rates of *O. marina* resulted from ingesting fewer *E. huxleyi* cells than

Table 3 Cell volumes (μm³) of *O. marina* fed non-infected and infected *E. huxleyi* over three days during experiment 4.

Treatment	Day	Replicate	Volume (μm³)
Om prey-depl	0		5586 ± 917
		A	4723 ± 1535
	1	B	5759 ± 1123
		C	5696 ± 1842
		A	4107 ± 1689
Om + Eh non-inf	2	B	3801 ± 660
		C	5602 ± 1045
		A	4675 ± 1141
	3	B	4038 ± 1319
		C	3949 ± 977
		A	5004 ± 1245
	1	B	4286 ± 1053
		C	4829 ± 1435
		A	6105 ± 462
Om + Eh inf	2	B	5561 ± 1483
		C	6977 ± 1371
		A	4267 ± 1218
	3	B	4478 ± 1184
		C	5527 ± 1956

Notes.

Om, *Oxyrrhis marina*; prey-depl, prey-depleted, i.e., not fed for three days; Eh non-inf, *Emiliania huxleyi* non-infected; Eh inf, *Emiliania huxleyi* infected with EhV-86.
Values are mean ± one standard deviation.

non-infected cells suggesting higher nutritional value of the infected *E. huxleyi* cells. Experiment 5 shows that the enhanced growth rates were not due to the ingestion of bacteria, virions, or DOM within the infected cultures. Furthermore, the fast growing *O. marina*, showed similar FA profile and cell size when compared to *O. marina* reared on non-infected algae suggesting that the quality of the dinoflagellates to higher trophic levels is unchanged. Consequently, the higher growth efficiencies of *O. marina* feeding on virally infected *E. huxleyi* cells suggest that viral infection of *E. huxleyi* increases the production of microzooplankton *O. marina*. These results suggest a shift in the "viral shunt" paradigm in which the flow of organic matter to higher trophic levels is enhanced by viral infection of algae rather than being short-circuited.

Oxyrrhis marina feed and grow on a wide range of protist prey types, as well as bacteria (*Jeong et al., 2008*) and DOM (*Lowe et al., 2011*). However, some prey enhance growth rates more than others (*Montagnes et al., 2011*). For example, virus-infected *E. huxleyi* cells supported higher *O. marina* growth than non-infected *E. huxleyi* cells, despite lower ingestion rates, suggesting higher nutritional value or higher assimilation efficiency of infected prey cells. It is worth noting that *O. marina* ingestion rates on virally infected *E. huxleyi* cultures might have been overestimated. A reduction in prey abundance due to viral lysis over each 24 h interval, prior to fresh-prey replenishment, during the experiments

might have led to temporarily reduced grazer-prey encounter and ingestion rates. Under such scenario *O. marina*'s growth per ingested infected cell would have been even larger than we estimated, adding further significance to our results. Consequently, our study would represent a conservative estimate of C transfer efficiency. This study also shows that *O. marina* only ingested bacteria when *E. huxleyi* cells were not available (or in very low abundance) and that ingestion of bacteria cells (and possibly EhV particles and/or DOM) alone does not support high growth rates compared to *E. huxleyi* cells even when bacteria are in very high concentrations (10^7 cells ml^{-1}).

Based on our measurements, the mechanisms underlying the lower ingestion rates of virally infected *E. huxleyi* cells and higher growth efficiency remain unknown. Calcification reduces digestion efficiency and predator growth (*Harvey, Bidle & Johnson, 2015*). In the environment, *E. huxleyi* cells lose their liths during an active viral infection (*Balch et al., 1993*; *Brussaard et al., 1996*; *Frada et al., 2008*; *Holligan et al., 1983*; *Jacquet et al., 2002*; *Trainic et al., 2018*). In this study we chose a non-calcifying *E. huxleyi* strain to uncouple the effects of calcification and prey size, on feeding and growth rates. Furthermore, we found no differences between C content in infected and non-infected *E. huxleyi* cells. In contrast, N content was slightly higher in non-infected cells. Nitrogen depletion in some prey cells causes *O. marina* to cease grazing, although the mechanisms remains unknown (*Flynn, Davidson & Cunningham, 1996*; *Martel, 2009*). However, C:N ratios in all of our *E. huxleyi* cultures (virus-infected or non-infected) were lower than 6.6, indicative that N was replete (*Davidson et al., 2005*; *Flynn, Davidson & Leftley, 1994*).

Large dsDNA viruses of eukaryotic algae, such as EhVs, have a high demand of C, N and P for the production of lipids, proteins, and nucleotides to support typical high burst sizes. Viral infection can modulate host metabolic pathways and nutrient uptake to fulfill the metabolic requirements of viral production (*Malitsky et al., 2016*; *Monier et al., 2017*; *Monier et al., 2012*; *Rosenwasser et al., 2014*; *Wilson, Carr & Mann, 1996*). The production of intermediary biomolecules and changes in *E. huxleyi*'s lipidome induced by infection with EhV-86 (*Evans et al., 2007*; *Evans et al., 2006*; *Evans, Pond & Wilson, 2009*; *Malitsky et al., 2016*; *Rosenwasser et al., 2014*; *Suzuki & Suzuki, 2006*) potentially increase the nutritional value of infected cells. During EhV infection, changes in biosynthesis pathways result in the production of more highly saturated FAs (*Evans, Pond & Wilson, 2009*; *Floge, 2014*; *Malitsky et al., 2016*) and the enhanced production of sphingolipids (*Pagarete et al., 2009*; *Rosenwasser et al., 2014*). It should be noted that the majority of these virus-induced alterations in lipid composition have been detected after prolonged infection (>24 h) of *E. huxleyi* cultures. At the relatively coarse level of detail in lipid profile carried out in the present study, only minor differences in FA composition were observed between non-infected *E. huxleyi* cultures and cultures that had been infected for 6 h (Table 2). This suggests that differences in FA composition between recently-infected and non-infected *E. huxleyi*, were not responsible for the differences in growth rates of *O. marina*. However, it is possible that the relatively small sample volume collected for FA analysis of *E. huxleyi* cells limited the resolution and detection of differences in FA between infected and non-infected *E. huxleyi* cells (*Evans, Pond & Wilson, 2009*; *Floge, 2014*; *Malitsky et al., 2016*). Alternatively the 6 h time frame used in this study may be

too short to measure significant changes in the FA profiles of infected cells. Alterations in lipid profile between infected and non-infected cells that were not apparent in our analysis (*Hunter et al., 2015*), may contribute to the higher growth efficiencies of *O. marina* fed virally infected prey cells.

An additional factor that influences the nutritional value of the phytoplankton prey is P concentration. In addition to providing a much needed resource for viral replication, P-rich phytoplankton cells increase grazing efficiency and secondary production in cladocerans (*Elser, Hayakawa & Urabe, 2001*; *Sterner, 1993*; *Urabe & Sterner, 1996*; *Urabe & Watanabe, 1992*). Low P availability reduces viral replication in *E. huxleyi* (*Bratbak, Egge & Heldal, 1993*) and other eukaryotic algae (*Maat et al., 2016*; *Wilson, Carr & Mann, 1996*), possibly by limiting the production of nucleic acids. It has been hypothesized that virally encoded putative phosphate transporters increase accumulation of P in host cells (*Monier et al., 2012*; *Wilson, Carr & Mann, 1996*). While to the best of our knowledge this has not been tested during the infection of *E. huxleyi* cells, most available EhV isolates, including EhV-86, carry an *E. huxleyi-* homolog putative phosphate repressible phosphate permease (PPRPP) gene (*Martínez Martínez, 2006*; *Nissimov et al., 2011*; *Nissimov et al., 2012*; *Wilson et al., 2005*), which we hypothesize led to higher P uptake in virally infected cells in our experiments. Additionally, the stoichiometric "light:nutrient hypothesis" poses that low supply of light relative to P yields more P-rich producers (i.e., low tissue C:P ratios) (*Sterner et al., 1997*); possibly due to the algae allocating high levels of P to light-harvesting cellular machinery and storing excess P intracellularly (*Hessen, Færøvig & Andersen, 2002*). In our study, *E. huxleyi* cells were grown in P-rich f/2-Si culture medium and both EhV-infected and non-infected cultures were kept under the same light conditions. In addition to the role of the PPRPP gene in P uptake, we hypothesize that virus-induced reduction in *E. huxleyi*'s photochemical efficiency from the early stages of EhV infection (*Gilg et al., 2016*) might also induce an increased P uptake and intracellular accumulation. While a reduction in photochemical efficiency might translate into lower C fixation rates, our results show that C content was not affected in infected compared to non-infected cells. Phosphorus content in infected and non-infected *E. huxleyi* cells and its impact on grazing warrants investigation in future studies.

E. huxleyi is an important food source at the base of the food chain and grazing pressure influences population and bloom dynamics (*Fileman, Cummings & Llewellyn, 2002*; *Olson & Strom, 2002*). Virus-induced mortality also plays a prominent role in bloom demise (*Bratbak, Egge & Heldal, 1993*; *Brussaard et al., 1996*; *Castberg et al., 2001*; *Lehahn et al., 2014*; *Martínez Martínez et al., 2007*) and diverts organic C away from upper trophic levels to the dissolved phase, which fuels the microbial loop—"viral shunt" (*Wilhelm & Suttle, 1999*). Our results suggest that viral infection also boosts microzooplankton production. High rates of viral infection can last from a few days (as in this study) to a few weeks during a natural *E. huxleyi* bloom progression (*Brussaard et al., 1996*; *Castberg et al., 2001*; *Martínez Martínez et al., 2007*), which could result in large differences in C flow through the food web. Extrapolating the results in our study, the enhanced growth rates of microzooplankton populations that feed on virally infected phytoplankton cells would lead to more organic C available for higher trophic levels. Thus, contrary to the idea that viral infection leads only

to the production of dissolved organic matter (*Wilhelm & Suttle, 1999*), viral infections at the base of the food chain may augment the flow of C to higher trophic levels as well as toward the microbial loop. To the best of our knowledge, the specific functional response of copepods ingestion of *O. marina* fed infected and non-infected *E. huxleyi* has yet to be investigated; however, the nutrition and reproduction rates are enhanced in copepods fed *O. marina* (grown on other phytoplankton diets) compared to copepods that feed directly on small phytoplankton cells (*Broglio et al., 2003*; *Chu, Lund & Podbesek, 2008*; *Parrish, French & Whiticar, 2012*; *Veloza, Chu & Tang, 2006*). Phytoplankton are considered the primary producers of essential FA long chain n-3 (LCn-3) PUFAs; however, heterotrophic dinoflagellates such as *O. marina* are also able to produce sterols and essential FAs (e.g., EPA (C20:5 n-3) and DHA (C22:6 n-3)) from lipid precursors (*Chu, Lund & Podbesek, 2008*; *Klein Breteler et al., 1999*; *Lund et al., 2008*; *Veloza, Chu & Tang, 2006*), which emphasizes the important role of certain microzooplankton groups in trophic upgrading and C transfer and highlights the need for a better quantitative understanding of the factors that influence microzooplankton grazing behavior and secondary production rates. Incorporating quantitative data for viral lysis and the effect of viral infection in grazing behavior and transfer efficiency into ecosystem models is essential for accurate budgeting of C flow throughout the food web in the global marine ecosystem. As a cautionary reminder, when interpreting these results it is important to note that *O. marina* is not typically found in open waters (*Yang, Jeong & Montagnes, 2011*) and is not likely to be a common natural predator of *E. huxleyi* cells. However *O. marina* is frequently used as a model predator in laboratory-based experiments because of its morphological similarity to a wide variety of heterotrophic and mixotrophic dinoflagellates and its plasticity in feeding behavior allow it to represent a broad range of marine dominant microzooplankton (*Lowe et al., 2011*; *Roberts et al., 2011*). Furthermore, several studies have shown that *O. marina* responds to various experimental stimuli in similar ways to that of other microzooplankton taxa (*Strom et al., 2003a*; *Strom et al., 2003b*; *Tillmann, 2004*). *E. huxleyi*'s true protozoan predators in nature have yet to be precisely identified (*Wolfe, 2000*).

A final consideration is that the lower ingestion rates of *O. marina* on *E. huxleyi* (strain CCMP374) cells infected with coccolithovirus EhV-86, compared to non-infected cells, are in contrast with an earlier study that used the same virus strain but a different *E. huxleyi* strain (CCMP 1516—non-calcifying) (*Evans & Wilson, 2008*). Strain-specific differences in the ingestion and clearance rates of *O. marina* feeding on *E. huxleyi* (*Harvey, Bidle & Johnson, 2015*) might have played a role in our findings. However, in light of our findings, the results from *Evans & Wilson (2008)* need to be revisited and revalidated and future studies should include multiple strains within a species (predator, prey, and/or virus) to test differences driven by intraspecific diversity. Importantly, future research is needed that focuses on a range of abundant and ecologically meaningful predator–prey-virus systems.

CONCLUSIONS

Viruses cause biochemical alterations to their *E. huxleyi* host cells to facilitate viral assembly (*Gilg et al., 2016*; *Malitsky et al., 2016*; *Rosenwasser et al., 2014*; *Suzuki & Suzuki, 2006*). The

data presented in this study show that changes in *E. huxleyi* as a result of viral infection cause higher growth efficiency and an increase in heterotrophic protist production. Despite the faster growth rates, we found no major difference in cell size, total FA content or FA profile of *O. marina* maintained on a diet of virally infected *E. huxleyi* cells during 3 days as compared with *O. marina* individuals reared on non-infected cells for the same period of time. Combined, these results suggest that during viral infection of *E. huxleyi,* the flow of C to higher trophic levels increases. Thus, in addition to the "viral shunt" hypothesis, these results suggest that virally infected *E. huxleyi* cells may also shunt more C to higher trophic levels. In order to gain a more comprehensive understanding of ocean ecosystem webs it is essential that we get quantitative knowledge of the relative magnitude of each pathway. The significance of our work is that, given the global scale and rapid dynamics of viral infections in the ocean, infection of primary producers is likely to be one of the compounding factors that influences the qualitative and quantitative flow of C in oceanic systems and determines overall efficiency of transfer to higher trophic levels.

ACKNOWLEDGEMENTS

ADDITIONAL INFORMATION AND DECLARATIONS

Competing Interests

The authors declare there are no competing interests.

Author Contributions

- Andrew G. Goode conceived and designed the experiments, performed the experiments, analyzed the data, prepared figures and/or tables, authored or reviewed drafts of the paper, approved the final draft.

- David M. Fields conceived and designed the experiments, performed the experiments, analyzed the data, contributed reagents/materials/analysis tools, authored or reviewed drafts of the paper, approved the final draft.
- Stephen D. Archer performed the experiments, analyzed the data, prepared figures and/or tables, authored or reviewed drafts of the paper, approved the final draft.
- Joaquín Martínez Martínez conceived and designed the experiments, performed the experiments, analyzed the data, contributed reagents/materials/analysis tools, prepared figures and/or tables, authored or reviewed drafts of the paper, approved the final draft.

Data Availability

The following information was supplied regarding data availability:

Raw data is provided in the Supplemental Information.

Supplemental Information

Supplemental information for this article can be found online at http://dx.doi.org/10.7717/peerj.6722#supplemental-information.

REFERENCES

Balch WM, Kilpatrick K, Holligan PM, Cucci T. 1993. Coccolith production and detachment by *Emiliania huxleyi* (Prymnesiophyceae). *Journal of Phycology* **29(5)**:566–575 DOI 10.1111/j.0022-3646.1993.00566.x.

Bratbak G, Egge JK, Heldal M. 1993. Viral mortality of the marine alga *Emiliania huxleyi* (Haptophyceae) and termination of algal blooms. *Marine Ecology Progress Series* **93**:39–48 DOI 10.3354/meps093039.

Broglio E, Jónasdóttir SH, Calbet A, Jakobsen HH, Saiz E. 2003. Effect of heterotrophic versus autotrophic food on feeding and reproduction of the calanoid copepod Acartia tonsa: relationship with prey fatty acid composition. *Aquatic Microbial Ecology* **31(3)**:267–278 DOI 10.3354/ame031267.

Brussaard CPD. 2004. Optimization of procedures for counting viruses by flow cytometry. *Applied and Environmental Microbiology* **70**:1506–1513 DOI 10.1128/AEM.70.3.1506-1513.2004.

Brussaard CPD, Kempers RS, Kop AJ, Riegman R, Heldal M. 1996. Virus-like particles in a summer bloom of *Emiliania huxleyi* in the North Sea. *Aquatic Microbial Ecology* **10(2)**:105–113 DOI 10.3354/ame010105.

Calbet A, Landry MR. 2004. Phytoplankton growth, microzooplankton grazing, and carbon cycling in marine systems. *Limnology and Oceanography* **49(1)**:51–57 DOI 10.4319/lo.2004.49.1.0051.

Castberg T, Larsen A, Sandaa RA, Brussaard CPD, Egge JK, Heldal M, Thyrhaug R, Van Hannen EJ, Bratbak G. 2001. Microbial population dynamics and diversity during a bloom of the marine coccolithophorid *Emiliania huxleyi* (Haptophyta). *Marine Ecology-Progress Series* **221**:39–46 DOI 10.3354/meps221039.

Chu FLE, Lund ED, Podbesek JA. 2008. Quantitative significance of n-3 essential fatty acid contribution by heterotrophic protists in marine pelagic food webs. *Marine Ecology Progress Series* **354**:85–95 DOI 10.3354/meps07215.

Davidson K, Roberts EC, Wilson AM, Mitchell E. 2005. The role of prey nutritional status in governing protozoan nitrogen regeneration efficiency. *Protist* **156(1)**:45–62 DOI 10.1016/j.protis.2004.10.001.

Edler L. 1979. Phytoplankton and chlorophyll: recommendations on methods for marine biological studies in the Baltic Sea. *Baltic Marine Biologists Publication* **5**:1–38.

Elser JJ, Hayakawa K, Urabe J. 2001. Nutrient limitation reduces food quality for zooplankton: daphnia response to seston phosphorus enrichment. *Ecology* **82(3)**:898–903 DOI 10.1890/0012-9658(2001)082[0898:NLRFQF]2.0.CO;2.

Evans C, Kadner SV, Darroch LJ, Wilson WH, Liss PS, Malin G. 2007. The relative significance of viral lysis and microzooplankton grazing as pathways of Dimethyl-sulfoniopropionate (DMSP) cleavage: an *Emiliania huxleyi* culture study. *Limnology and Oceanography* **52(3)**:1036–1045 DOI 10.4319/lo.2007.52.3.1036.

Evans C, Malin G, Mills GP, Wilson WH. 2006. Viral infection of *Emiliania huxleyi* (Prymnesiophyceae) leads to elevated production of reactive oxygen species. *Journal of Phycology* **42(5)**:1040–1047 DOI 10.1111/j.1529-8817.2006.00256.x.

Evans C, Pond DW, Wilson WH. 2009. Changes in Emiliania huxleyi fatty acid profiles during infection with E. huxleyi virus 86: physiological and ecological implications. *Aquatic Microbial Ecology* **55**:219–228 DOI 10.3354/ame01295.

Evans C, Wilson WH. 2008. Preferential grazing of Oxyrrhis marina on virus infected Emiliania huxleyi. *Limnology and Oceanography* **53(3)**:2035–2040 DOI 10.4319/lo.2008.53.5.2035.

Fileman ES, Cummings DG, Llewellyn CA. 2002. Microplankton community structure and the impact of microzooplankton grazing during an Emiliania huxleyi bloom, off the Devon coast. *Journal of the Marine Biological Association of the United Kingdom* **82(2)**:359–368 DOI 10.1017/S0025315402005593.

Floge S. 2014. Virus infections of eukaryotic viruses. PhD thesis, University of Maine.

Flynn KJ, Davidson K, Cunningham A. 1996. Prey selection and rejection by a microflagellate; implications for the study and operation of microbial food webs. *Journal of Experimental Marine Biology and Ecology* **196(1–2)**:357–372 DOI 10.1016/0022-0981(95)00140-9.

Flynn KJ, Davidson K, Leftley JW. 1994. Carbon-nitrogen relations at whole-cell and free-amino-acid levels during batch growth of Isochrysis galbana (Prymnesiophyceae) under conditions of alternating light and dark. *Marine Biology* **118(2)**:229–237 DOI 10.1007/bf00349789.

Frada M, Probert I, Allen MJ, Wilson WH, De Vargas C. 2008. The 'Cheshire Cat' escape strategy of the coccolithophore Emiliania huxleyi in response to viral infection. *Proceedings of the National Academy of Sciences of the United States of America* **105(41)**:15944–15949 DOI 10.1073/pnas.0807707105.

Frost BW. 1972. Effects of size and concentration of food particles on the feeding behavior of the marine planktonic copepod *Calanus pacificus. Limnology and Oceanography* **17**(**6**):805–815 DOI 10.4319/lo.1972.17.6.0805.

Gilg IC, Archer SD, Floge SA, Fields DM, Vermont AI, Leavitt AH, Wilson WH, Martínez Martínez J. 2016. Differential gene expression is tied to photochemical efficiency reduction in virally infected Emiliania huxleyi. *Marine Ecology Progress Series* **555**:13–27 DOI 10.3354/meps11805.

Guillard RRL. 1975. Culture of phytoplankton for feeding marine invertebrates. In: Smith WL, Chanley MH, eds. *Culture of marine invertebrate animals.* New York: Plenum Press, 29–60.

Harvey EL, Bidle KD, Johnson MD. 2015. Consequences of strain variability and calcification in Emiliania huxleyi on microzooplankton grazing. *Journal of Plankton Research* **37**(**6**):1137–1148 DOI 10.1093/plankt/fbv081.

Hessen DO, Færøvig PJ, Andersen T. 2002. Light, nutrients, ans P:C ratios in algae: grazer performance related to food quality and quantity. *Ecology* **83**(**7**):1886–1898 DOI 10.1890/0012-9658(2002)083[1886:LNAPCR]2.0.CO;2.

Holligan PM, Fernandez E, Aiken J, Balch WM, Boyd P, Burkill PH, Finch M, Groom SB, Malin G, Muller K, Purdie DA, Robinson C, Trees CC, Turner SM, Vanderwal P. 1993. A biogeochemical study of the coccolithophore, *Emiliania huxleyi*, in the North-Atlantic. *Global Biogeochem Cy* **7**:879–900 DOI 10.1029/93GB01731.

Holligan PM, Viollier M, Harbour DS, Camus P, Champagnephilippe M. 1983. Satellite and ship studies of coccolithophore production along a continental-shelf edge. *Nature* **304**:339–342 DOI 10.1038/304339a0.

Hunter JE, Frada MJ, Fredricks HF, Vardi A, Van Mooy BAS. 2015. Targeted and untargeted lipidomics of Emiliania huxleyi viral infection and life cycle phases highlights molecular biomarkers of infection, susceptibility, and ploidy. *Frontiers in Marine Science* **2**:81 DOI 10.3389/fmars.2015.00081.

Jacobsen A, Grahl-Nielsen O, Magnesen T. 2012. Effects of reduced diameter of bag cultures on content of essential fatty acids and cell density in a continuous algal production system. *Journal of Applied Phycology* **24**(**1**):109–116 DOI 10.1007/s10811-011-9655-6.

Jacquet S, Heldal M, Iglesias-Rodriguez D, Larsen A, Wilson W, Bratbak G. 2002. Flow cytometric analysis of an *Emiliana huxleyi* bloom terminated by viral infection. *Aquatic Microbial Ecology* **27**(**2**):111–124 DOI 10.3354/ame027111.

Jeong HJ, Seong KA, Yoo YD, Kim TH, Kang NS, Kim S, Park JY, Kim JS, Kim GH, Song JY. 2008. Feeding and grazing impact by small marine heterotrophic Dinoflagellates on heterotrophic bacteria. *Journal of Eukaryotic Microbiology* **55**(**4**):271–288 DOI 10.1111/j.1550-7408.2008.00336.x.

Klein Breteler WCM, Schogt N, Baas M, Schouten S, Kraay GW. 1999. Trophic upgrading of food quality by protozoans enhancing copepod growth: role of essential lipids. *Marine Biology* **135**(**1**):191–198 DOI 10.1007/s002270050616.

Lehahn Y, Koren I, Schatz D, Frada M, Sheyn U, Boss E, Efrati S, Rudich Y, Trainic M, Sharoni S, Laber C, DiTullio Giacomo R, Coolen Marco JL, Martins Ana M,

Van Mooy Benjamin AS, Bidle Kay D, Vardi A. 2014. Decoupling physical from biological processes to assess the impact of viruses on a mesoscale algal bloom. *Current Biology* **24(17)**:2041–2046 DOI 10.1016/j.cub.2014.07.046.

Lowe CD, Martin LE, Roberts EC, Watts PC, Wootton EC, Montagnes DJS. 2011. Collection, isolation and culturing strategies for Oxyrrhis marina. *Journal of Plankton Research* **33(4)**:569–578 DOI 10.1093/plankt/fbq161.

Lund ED, Chu F-LE, Harvey E, Adlof R. 2008. Mechanism(s) of long chain n-3 essential fatty acid production in two species of heterotrophic protists: Oxyrrhis marina and Gyrodinium dominans. *Marine Biology* **155(1)**:23–36 DOI 10.1007/s00227-008-1003-2.

Maat DS, Brussaard CPD. 2016. Both phosphorus- and nitrogen limitation constrain viral proliferation in marine phytoplankton. *Aquatic Microbial Ecology* **77(2)**:87–97 DOI 10.3354/ame01791.

Maat DS, Van Bleijswijk JDL, Witte HJ, Brussaard CPD. 2016. Virus production in phosphorus-limited Micromonas pusilla stimulated by a supply of naturally low concentrations of different phosphorus sources, far into the lytic cycle. *FEMS Microbiology Ecology* **92(9)**:fiw136–fiw136 DOI 10.1093/femsec/fiw136.

Mackinder LCM, Worthy CA, Biggi G, Hall M, Ryan KP, Varsani A, Harper G, Wilson WH, Brownlee C, Schroeder DC. 2009. A unicelular algal virus, *Emiliania huxleyi* virus 86, exploits an animal-like infection strategy. *Journal of General Virology* **90**:2306–2316 DOI 10.1099/vir.0.011635-0.

Malitsky S, Ziv C, Rosenwasser S, Zheng S, Schatz D, Porat Z, Ben-Dor S, Aharoni A, Vardi A. 2016. Viral infection of the marine alga Emiliania huxleyi triggers lipidome remodeling and induces the production of highly saturated triacylglycerol. *New Phytologist* **210(1)**:88–96 DOI 10.1111/nph.13852.

Marie D, Brussaard CPD, Thyrhaug R, Bratbak G, Vaulot D. 1999. Enumeration of marine viruses in culture and natural samples by flow cytometry. *Applied and Environmental Microbiology* **65**:45–52.

Martel CM. 2009. Conceptual bases for prey biorecognition and feeding selectivity in the microplanktonic marine phagotroph Oxyrrhis marina. *Microbial Ecology* **57(4)**:589–597 DOI 10.1007/s00248-008-9421-8.

Martínez Martínez J. 2006. Molecular ecology of marine algal viruses. PhD thesis, University of Plymouth.

Martínez Martínez J, Norland S, Thingstad F, Schroeder DC, Bratbak G, Wilson WH, Larsen A. 2006. Variability in microbial population dynamics between similarly perturbed mesocosms. *Journal of Plankton Research* **28(8)**:783–791 DOI 10.1093/plankt/fbl010.

Martínez Martínez J, Poulton NJ, Stepanauskas R, Sieracki ME, Wilson WH. 2011. Targeted Sorting of Single Virus-Infected Cells of the Coccolithophore *Emiliania huxleyi*. *PLOS ONE* **6(7)**:e22520 DOI 10.1371/journal.pone.0022520.

Martínez Martínez J, Schroeder DC, Larsen A, Bratbak G, Wilson WH. 2007. Molecular dynamics of *Emiliania huxleyi* and cooccurring viruses during two

separate mesocosm studies. *Applied Environmental Microbiology* **73**:554–562 DOI 10.1128/AEM.00864-06.

Meier S, Mjøs SA, Joensen H, Grahl-Nielsen O. 2006. Validation of a one-step extraction/methylation method for determination of fatty acids and cholesterol in marine tissues. *Journal of Chromatography A* **1104(1–2)**:291–298 DOI 10.1016/j.chroma.2005.11.045.

Menden-Deuer S, Lessard EJ. 2000. Carbon to volume relationships for dinoflagellates, diatoms, and other protist plankton. *Limnology and Oceanography* **45(3)**:569–579 DOI 10.4319/lo.2000.45.3.0569.

Menden-Deuer S, Lessard EJ, Satterberg J. 2001. Effect of preservation on dinoflagellate and diatom cell volume and consequences for carbon biomass predictions. *Marine Ecology Progress Series* **222**:41–50 DOI 10.3354/meps222041.

Mojica KDA, Brussaard CPD. 2014. Factors affecting virus dynamics and microbial host–virus interactions in marine environments. *FEMS Microbiology Ecology* **89(3)**:495–515 DOI 10.1111/1574-6941.12343.

Monier A, Chambouvet A, Milner DS, Attah V, Terrado R, Lovejoy C, Moreau H, Santoro AE, Derelle É, Richards TA. 2017. Host-derived viral transporter protein for nitrogen uptake in infected marine phytoplankton. *Proceedings of the National Academy of Sciences of the United States of America* **114(36)**:e7489–E7498 DOI 10.1073/pnas.1708097114.

Monier A, Welsh RM, Gentemann C, Weinstock G, Sodergren E, Armbrust EV, Eisen JA, Worden AZ. 2012. Phosphate transporters in marine phytoplankton and their viruses: cross-domain commonalities in viral-host gene exchanges. *Environmental Microbiology* **14(1)**:162–176 DOI 10.1111/j.1462-2920.2011.02576.x.

Montagnes DJS, Lowe CD, Martin L, Watts PC, Downes-Tettmar N, Yang Z, Roberts EC, Davidson K. 2011. Oxyrrhis marina growth, sex and reproduction. *Journal of Plankton Research* **33(4)**:615–627 DOI 10.1093/plankt/fbq111.

Nissimov JI, Worthy CA, Rooks P, Napier JA, Kimmance SA, Henn MR, Ogata H, Allen MJ. 2011. Draft genome sequence of the coccolithovirus Emiliania huxleyi Virus 203. *Journal of Virology* **85**:13468–13469 DOI 10.1128/jvi.06440-11.

Nissimov JI, Worthy CA, Rooks P, Napier JA, Kimmance SA, Henn MR, Ogata H, Allen MJ. 2012. Draft genome sequence of the coccolithovirus Emiliania huxleyi Virus 202. *Journal of Virology* **86**:2380–2381 DOI 10.1128/jvi.06863-11.

Olson MB, Strom SL. 2002. Phytoplankton growth, microzooplankton herbivory and community structure in the southeast Bering Sea: insight into the formation and temporal persistence of an Emiliania huxleyi bloom. *Deep-Sea Research Part II—Topical Studies in Oceanography* **49(26)**:5969–5990brk DOI 10.1016/S0967-0645(02)00329-6.

Pagarete A, Allen MJ, Wilson WH, Kimmance SA, Vargas CDe. 2009. Host–virus shift of the sphingolipid pathway along an Emiliania huxleyi bloom: survival of the fattest. *Environmental Microbiology* **11(11)**:2840–2848brk DOI 10.1111/j.1462-2920.2009.02006.x.

Parrish CC, French VM, Whiticar MJ. 2012. Lipid class and fatty acid composition of copepods (Calanus finmarchicus, C. glacialis, Pseudocalanus sp. Tisbe furcata and Nitokra lacustris) fed various combinations of autotrophic and heterotrophic protists. *Journal of Plankton Research* **34(5)**:356–375 DOI 10.1093/plankt/fbs003.

Roberts EC, Wootton EC, Davidson K, Jeong HJ, Lowe CD, Montagnes DJS. 2011. Feeding in the dinoflagellate Oxyrrhis marina: linking behaviour with mechanisms. *Journal of Plankton Research* **33(4)**:603–614 DOI 10.1093/plankt/fbq118.

Rosenwasser S, Mausz MA, Schatz D, Sheyn U, Malitsky S, Aharoni A, Weinstock E, Tzfadia O, Ben-Dor S, Feldmesser E, Pohnert G, Vardi A. 2014. Rewiring Host Lipid Metabolism by Large Viruses Determines the Fate of Emiliania huxleyi, a Bloom-Forming Alga in the Ocean. *The Plant Cell Online* **26**:2689–2707 DOI 10.1105/tpc.114.125641.

Schneider CA, Rasband WS, Eliceiri KW. 2012. NIH Image to ImageJ: 25 years of image analysis. *Nature Methods* **9**:671–675 DOI 10.1038/nmeth.2089.

Sherr EB, Sherr BF. 2002. Significance of predation by protists in aquatic microbial food webs. *Antonie Van Leeuwenhoek International Journal of General and Molecular Microbiology* **81(1–4)**:293–308 DOI 10.1023/a:1020591307260.

Sherr EB, Sherr BF. 2009. Capacity of herbivorous protists to control initiation and development of mass phytoplankton blooms. *Aquatic Microbial Ecology* **57(3)**:253–262 DOI 10.3354/ame01358.

Sterner RW. 1993. Daphnia growth on varying quality of scenedesmus: mineral limitation of zooplankton. *Ecology* **74(8)**:2351–2360 DOI 10.2307/1939587.

Sterner RW, Elser JJ, Fee EJ, Guildford SJ, Chrzanowski TH. 1997. The light: nutrient ratio in lakes: the balance of energy and materials affects ecosystem structure and process. *The American Naturalist* **150(6)**:663–684 DOI 10.1086/286088.

Strom SL, Brainard MA, Holmes JL, Olson MB. 2001. Phytoplankton blooms are strongly impacted by microzooplankton grazing in coastal North Pacific waters. *Marine Biology* **138(2)**:355–368 DOI 10.1007/s002270000461.

Strom S, Wolfe G, Holmes J, Stecher H, Shimeneck C, Sarah L. 2003a. Chemical defense in the microplankton I: feeding and growth rates of heterotrophic protists on the DMS-producing phytoplankter Emiliania huxleyi. *Limnology and Oceanography* **48(1)**:217–229 DOI 10.4319/lo.2003.48.1.0217.

Strom S, Wolfe G, Slajer A, Lambert S, Clough J. 2003b. Chemical defense in the microplankton II: inhibition of protist feeding by β-dimethylsulfoniopropionate (DMSP). *Limnology and Oceanography* **48(1)**:230–237 DOI 10.4319/lo.2003.48.1.0230.

Suttle CA. 1994. The significance of viruses to mortality in aquatic microbial communities. *Microbial Ecology* **28(2)**:237–243 DOI 10.1007/BF00166813.

Suttle C. 2005. Viruses in the sea. *Nature* **437**:356–361 DOI 10.1038/nature04160.

Suzuki T, Suzuki Y. 2006. Virus infection and lipid rafts. *Biological and Pharmaceutical Bulletin* **29(8)**:1538–1541 DOI 10.1248/bpb.29.1538.

Thingstad TF. 2000. Elements of a theory for the mechanisms controlling abundance, diversity, and biogeochemical role of lytic bacterial viruses in aquatic systems. *Limnology and Oceanography* **45**:1320–1328 DOI 10.4319/lo.2000.45.6.1320.

Tillmann U. 2004. Interactions between Planktonic Microalgae and Protozoan Grazers1. *Journal of Eukaryotic Microbiology* **51(2)**:156–168 DOI 10.1111/j.1550-7408.2004.tb00540.x.

Trainic M, Koren I, Sharoni S, Frada M, Segev L, Rudich Y, Vardi A. 2018. Infection dynamics of a bloom-forming alga and its virus determine airborne coccolith emission from seawater. *iScience* **6**:327–335 DOI 10.1016/j.isci.2018.07.017.

Urabe J, Sterner RW. 1996. Regulation of herbivore growth by the balance of light and nutrients. *Proceedings of the National Academy of Sciences of the United States of America* **93(16)**:8465–8469 DOI 10.1073/pnas.93.16.8465.

Urabe J, Watanabe Y. 1992. Possibility of N or P limitation for planktonic cladocerans: an experimental test. *Limnology and Oceanography* **37(2)**:244–251 DOI 10.4319/lo.1992.37.2.0244.

Van Hannen EJ, Zwart G, Van Agterveld MP, Gons HJ, Ebert J, Laanbroek HJ. 1999. Changes in bacterial and eukaryotic community structure after mass lysis of filamentous cyanobacteria associated with viruses. *Applied and Environmental Microbiology* **65**:795–801.

Veloza AJ, Chu F-LE, Tang KW. 2006. Trophic modification of essential fatty acids by heterotrophic protists and its effects on the fatty acid composition of the copepod Acartia tonsa. *Marine Biology* **148(8)**:779–788 DOI 10.1007/s00227-005-0123-1.

Vermont A, Martínez Martínez J, Waller J, Gilg I, Leavitt A, Floge S, Archer S, Wilson W, Fields D. 2016. Virus infection of Emiliania huxleyi deters grazing by the copepod Acartia tonsa. *Journal of Plankton Research* **38(5)**:1194–1205 DOI 10.1093/plankt/fbw064.

Weitz JS, Stock CA, Wilhelm SW, Bourouiba L, Coleman ML, Buchan A, Follows MJ, Fuhrman JA, Jover LF, Lennon JT, Middelboe M, Sonderegger DL, Suttle CA, Taylor BP, Thingstad TFrede, Wilson WH, Wommack KEric. 2015. A multitrophic model to quantify the effects of marine viruses on microbial food webs and ecosystem processes. *The ISME Journal* **9(6)**:1352–1364 DOI 10.1038/ismej.2014.220.

Wilhelm SW, Suttle CA. 1999. Viruses and nutrient cycles in the sea. Viruses play critical roles in the structure and function of aquatic food webs. *Bioscience* **49**:781–788 DOI 10.2307/1313569.

Wilson WH, Carr NG, Mann NH. 1996. The effect of phosphate status on the kinetics of cyanophage infection in the oceanic cyanobacterium *Synechococcus* sp WH7803. *Journal of Phycology* **32**:506–516 DOI 10.1111/j.0022-3646.1996.00506.x.

Wilson WH, Schroeder DC, Allen MJ, Holden M, Parkhill J, Barrell BG, Churcher C, Hamlin N, Mungall K, Norbertczak H, Quail MA, Price CC, Rabbinowitsch E, Walker D, Craigon M, Roy D, Ghazal P. 2005. Complete genome sequence and lytic phase transcription profile of a *Coccolithovirus*. *Science* **309(5737)**:1090–1092 DOI 10.1126/science.1113109.

Wilson WH, Tarran GA, Schroeder D, Cox M, Oke J, Malin G. 2002. Isolation of viruses responsible for the demise of an *Emiliania huxleyi* bloom in the English Channel. *Journal of the Marine Biological Association of the United Kingdom* **82(3)**:369–377 DOI 10.1017/S002531540200560X.

Wolfe G. 2000. The chemical defense ecology of marine unicellular plankton: constraints, mechanisms, and impacts. *The Biological Bulletin* **198**:225–244 DOI 10.2307/1542526.

Yang Z, Jeong HJ, Montagnes DJS. 2011. The role of Oxyrrhis marina as a model prey: current work and future directions. *Journal of Plankton Research* **33**:665–675 DOI 10.1093/plankt/fbq112.